photonics

MDPI

Article

Desensitization Design Method for Freeform TMA Optical Systems Based on Initial Structure Screening

Zichang Qin [1,2], Yunsheng Qi [1,2], Chengming Ren [1,2], Xiaodong Wang [1] and Qingyu Meng [1,*]

[1] Changchun Institute of Optics, Fine Mechanics and Physics, Chinese Academy of Sciences, Changchun 130033, China; qinzichang@ciomp.ac.cn (Z.Q.); qiyunsheng21@mails.ucas.ac.cn (Y.Q.); renchengming21@mails.ucas.ac.cn (C.R.); wxd@ciomp.ac.cn (X.W.)
[2] University of the Chinese Academy of Sciences, Beijing 100049, China
* Correspondence: mengqy@ciomp.ac.cn

Abstract: Achieving aberration correction can improve the imaging quality of an optical system, and reducing the error sensitivity of system can improve the realizability of the system. In order to obtain an off-axis three-mirror optical system with high image quality and low error sensitivity, a design method is proposed which obtains the initial structure of the three-mirror anastigmatic (TMA) optical system with low error sensitivity through a nondominated sorting genetic algorithm II (NSGA-II). Combining the comprehensive evaluation function of image quality and error sensitivity, this method iteratively selects multiple freeform surface types to determine the combination with the lowest error sensitivity and obtains the freeform TMA optical system with optimal overall performance. A freeform TMA optical system is designed by the method proposed in this paper, and the error sensitivity of the optical system is analyzed. The results show that the image quality of the freeform optical system is effectively improved and the error sensitivity is effectively reduced with the same error applied, which verifies the correctness and practicality of the method.

Keywords: TMA optical systems; desensitization design method; freeform surface

Citation: Qin, Z.; Qi, Y.; Ren, C.; Wang, X.; Meng, Q. Desensitization Design Method for Freeform TMA Optical Systems Based on Initial Structure Screening. *Photonics* **2022**, *9*, 544. https://doi.org/10.3390/photonics9080544

Received: 12 July 2022
Accepted: 29 July 2022
Published: 3 August 2022

1. Introduction

TMA optical systems can achieve a larger relative aperture, larger field of view (FOV), and higher imaging quality when combined with freeform optical surfaces with strong aberration correction capability [1–5]. High-performance optical systems are up-and-coming and have been implemented [6–8]. However, due to the non-rotational symmetry of the system, the complexity and difficulty of the processing and alignment of freeform TMA optical systems are more significant, and the sensitivity of optical element position errors is also higher [9–11]. Therefore, it is of great significance for the high-performance imaging design and realization of the freeform TMA optical system if the error sensitivity can be reduced while achieving the high-performance optical system.

We believe that two aspects of the desensitization design of freeform optical systems are essential: the first is to obtain the initial structure of the optical system with low error sensitivity, and the second is the desensitization optimization of the freeform optical system. The close combination of the two aspects is an effective way to obtain a freeform TMA optical system with low error sensitivity.

Obtaining the initial structure is the beginning of optical design. An excellent initial structure plays a critical role in the optical system's subsequent optimization and final performance realization. The traditional initial structure solution for optical systems mainly focuses on the object-image relationship and aberration correction. In recent years, some new initial structure solution methods have been reported for freeform systems, such as the Wassermann-Wolf differential-equations method [12–14], the simultaneous multi-surface design method [15,16], and the design method based on point-by-point construction and iteration [17–20], etc., However, not many publicly reported initial structure solution

methods have taken the performance of optical system error sensitivity as the core of the investigation. Some optical system initially structure solutions on error sensitivity, primarily applying damped least squares (DLS) to obtain local minima rather than optimal global solutions [21–23]. Some other solution methods are mainly qualitative and lack quantitative evaluation indicators.

For the desensitization optimization of optical systems, the usual methods are the global optimization method, parameter control method, and freeform surface optimization method. The global optimization method is to optimize and iterate on a large sample of optical systems that have completed image quality optimization and to select systems with better tolerance robustness [24–26], which is a qualitative method. The parameter control method is based on the optical system parameters obtained from theoretical studies with a clear regular or quantitative relationship with the error sensitivity. In optimization, process desensitization is achieved by direct or indirect control of these parameters [10,27–30]. This method is a quantitative desensitization design method that can visually regulate specific values associated with the error sensitivity of the optical system. In recent years, some other studies have shown that optical systems applied to certain freeform surfaces have lower error sensitivity than those applied aspheric surfaces [31–33], which leaves the application of freeform surfaces to improve the imaging performance of optical systems and the potential of error sensitivity to be exploited.

In light of the above discussion, this paper proposes a desensitization design method for freeform TMA optical systems based on initial structure screening. The method combines the features of the global optimization method, parameter control method, and freeform optimization method and considers the advantages of multiple design methods. First, the initial structure of the TMA optical system is selected by the NSGA-II, and the freeform surface is introduced into the conic TMA system in order to improve the system performance. The characteristic parameters affecting the error sensitivity of the freeform optical system are controlled based on the proposed quantitative evaluation function of the error sensitivity. In order to exploit the desensitization potential of the freeform surface, the combination of multiple types of freeform surfaces is screened and optimized to obtain the best combination of surface types considering the optical system's imaging quality and error sensitivity. Finally, the desensitization design of the free-form optical system is produced. In order to verify the effectiveness of the desensitization design method, a freeform TMA optical system with a focal length of 100 mm, an *F*-number of 5, and a FOV of $3^\circ \times 3^\circ$ is used as an example for the desensitization design. The error sensitivity analysis with the counterpart conic optical system shows that the freeform optical system obtained by applying the desensitization design method has a significant improvement in the image quality and error sensitivity performance with the same error applied.

2. Error Sensitivity Evaluation Function for Freeform Surfaces

Tilt is an important manifestation of the position error of optical elements [34]. It mainly causes asymmetric aberrations such as astigmatism, which is difficult to compensate for the image quality by defocus. Therefore, the tilt error has been taken as an essential research object in the theoretical research of the error sensitivity of optical systems.

A tilt sensitivity evaluation function was proposed in our previous study and effectively used to evaluate the error sensitivity of the conic TMA optical system. The method is improved to evaluate and optimize the error sensitivity of the freeform TMA optical system by combining the method with ray sampling.

The error sensitivity evaluation function is the core of the optical system desensitization design. In order to establish an effective evaluation function, the first is to investigate the clear mathematical relationship between the internal parameters of the optical system and the error sensitivity under the condition of tilt error perturbation, and then to control these parameters to achieve the desensitization in the subsequent desensitization design. Based on the geometric ray-tracing method, the error sensitivity of the optical system is manifested by the variation of optical path difference (OPD). By deriving the variation of

OPD (ΔOPD) of any ray of the optical system before and after being disturbed by tilt, it is concluded that the larger the slope of the tangent line at the intersection of the ray and the mirror is, the smaller the ΔOPD due to the error is, which means the error sensitivity is lower [30]. Therefore, the tangent slope at the intersection of ray and mirror is determined to be a pivotal factor in characterizing the error sensitivity of the optical system, and a tilt error sensitivity evaluation function with the tangent slope as the core is proposed accordingly.

The schematic diagram of ray propagation at the intersection of the optical element is shown in Figure 1. The intersection of the incidence ray and the mirror is *N*. The tangent line to the mirror is made at point *N*. The slope of the tangent line is defined as *K*.

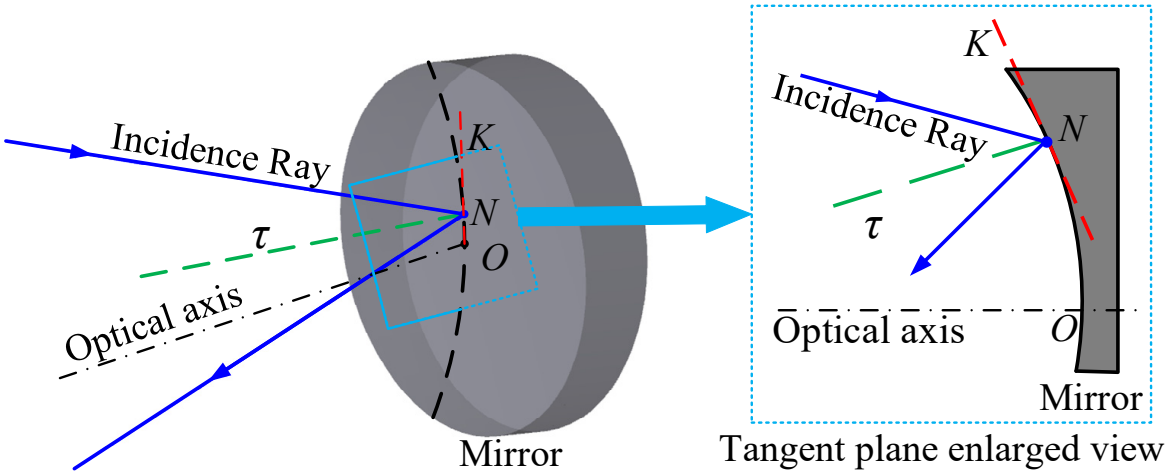

Figure 1. Schematic diagram of ray propagation at the intersection of incidence ray and the mirror.

The tangent slope *K* at the intersection of ray and mirror is inversely proportional to the tilt error sensitivity of the optical system, so the larger the value of *K* in the desensitization design is, the lower error sensitivity is. However, the maximum value of *K* cannot be obtained as a tangent function, leading to the inability to set a suitable threshold. Based on the analysis of the optimization function, the optimization process is usually to obtain the minimum value of the optimization function. Therefore, in order to facilitate the setting of the error sensitivity threshold, the absolute value of the reciprocal of *K* is defined as τ, and the error sensitivity evaluation function is constructed [34].

Define the mirror tilt error sensitivity evaluation function as $SEN_{Surface}$:

$$SEN_{Surface} = \sqrt{\frac{\sum_{k=1}^{NOF} \tau_k^2}{k}}, \quad (1)$$

where *k* is the serial number of the field and *NOF* is the number of FOV sampling points.

Define the optical system tilt error sensitivity evaluation function as SEN_{System}:

$$SEN_{System} = \frac{\sum_{i=1}^{3} SEN_{Surface}}{k}, \quad (2)$$

where *i* is the serial number of the surface.

Since freeform surfaces do not have rotational symmetry, it is difficult to effectively control the error sensitivity of an optical system by analyzing only one ray. Therefore, it is necessary to extend the application of the error sensitivity evaluation function for freeform optical systems and an error sensitivity evaluation method applicable to any freeform surface is proposed.

In the error sensitivity evaluation method based on ray tracing, aiming at the footprint of a mirror through a certain FOV, the "Ring-Arm" sampling method with high sampling

density reflects the idea of global desensitization from the parts to the whole, and achieves the purpose of reducing the comprehensive error sensitivity of the TMA optical system.

The sampling method of "Ring-Arm" is used, and $NOR \times NOA$ sampling points are selected. The number of selected Rings is *NOR*, and the number of selected Arms is *NOA*. The Rings and Arms are chosen as follows—Ring is defined as follows: Ring # represents the serial number of the Ring, from the center outward as light purple Ring 1, green Ring 2, blue Ring 3, black Ring... representing the possible Rings, dark red Ring *NOR*. The Arms are defined as follows: Arm # represents the serial number of the Arm, starting from the meridian +90° direction as Arm 1, and sorted counterclockwise as Arm 2, Arm 3, Arm... representing the possible Arms, Arm NOA. For example, Ring 3, Arm2 corresponds to the location of the reference point as shown by the red arrow in Figure 2.

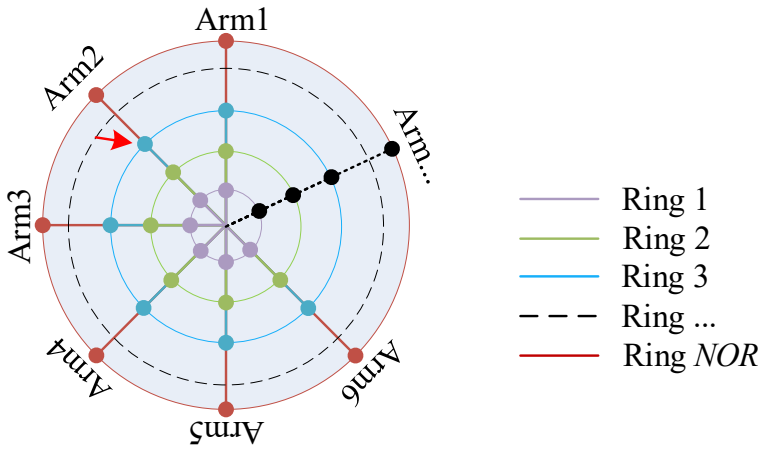

Figure 2. Reference point selection diagram.

At each sampling point, the tangent slope of the intersection of the ray and the mirror is defined as *Ku*,*v*. The error sensitivity of one freeform mirror corresponding to a single FOV is calculated first, and then the average of the error sensitivity of freeform TMA optical system corresponding to each FOV is calculated as the comprehensive error sensitivity evaluation function.

Error sensitivity for a single FOV, a single freeform mirror is defined as *SENF*:

$$SENF = \sqrt{\frac{\sum_{u=1}^{NOR}\sum_{v=1}^{NOA}\tau_{u,v}^2}{NOR \times NOA}}, \tag{3}$$

where, u is the serial number of the Ring, v is the serial number of the Arm.

Error sensitivity for all FOVs corresponding to the freeform TMA optical system is defined as $SENF_{System}$:

$$SENF_{System} = \frac{\sum_{k=1}^{NOF}\sqrt{\sum_{i=1}^{3}\frac{SENF_i^2}{3}}}{NOF}, \tag{4}$$

3. Design Method

3.1. Initial Structure Construction

In this paper, the NSGA-II algorithm is used to automatically calculate the initial system structure parameters. The NSGA-II algorithm, proposed by Srinivas and Deb in 2000, is one of the most popular multi-objective genetic algorithms, which reduces the complexity of non-inferiority ranking genetic algorithms and has the advantages of fast operation and good convergence of the solution set, making it a benchmark for the performance of other multi-objective optimization algorithms [35]. Minimizing two or more value functions by using the NSGA-II algorithm will result in a compromised set of solutions (Pareto solutions) rather than just the single solution obtained in single-objective

optimization algorithms. The researcher can decide the importance of two or more value functions through the analysis and thus select the desired result among the Pareto solutions. The specific process of the NSGA-II algorithm is not described in detail here. In the design of the TMA optical system, the layout of the three-mirror system is shown in Figure 3.

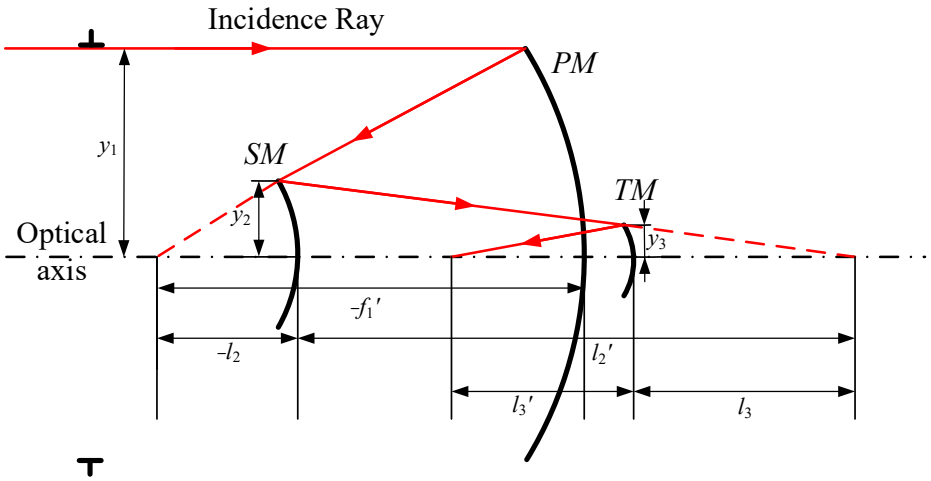

Figure 3. Layout of three-mirror optical system.

The system consists of three mirrors: primary mirror (*PM*), secondary mirror (*SM*), and triple mirror (*TM*). y_1, y_2, and y_3 are the half-apertures of *PM*, *SM*, and *TM*; the objective distance of the *PM* is infinity; l_2 and l_3 are the objective distances of the *SM* and *TM*, respectively; f_1', l_2', and l_3' are the image distances of the *PM*, *SM*, and *TM*, respectively. The blocking ratios of *SM* to *PM* and *TM* to *SM* are α_1 and α_2, respectively the magnifications of *SM* and *TM* are β_1 and β_2, respectively, and the conic coefficients of each mirror are ${e_1}^2$, ${e_2}^2$, and ${e_3}^2$, respectively. Where

$$\begin{cases} \alpha_1 = \frac{l_2}{f_1'} \approx \frac{y_2}{y_1} \\ \alpha_2 = \frac{l_3}{l_2'} \approx \frac{y_3}{y_2} \end{cases}, \begin{cases} \beta_1 = \frac{l_2'}{l_2} \\ \beta_2 = \frac{l_3'}{l_3} \end{cases}, \tag{5}$$

Firstly, two blocking ratios (α_1, α_2), two magnifications (β_1, β_2), and three conic coefficients (${e_1}^2$, ${e_2}^2$, ${e_3}^2$) are set as variables. The initial structure of TMA optical system can be obtained by introducing the parameters into Equation (6).

Assuming that the focal length of the three mirror system is f', the expressions of the curvature radii of *PM*, *SM*, and *TM* and their corresponding thicknesses are calculated according to the paraxial optical theory as follows:

$$\begin{cases} R_1 = \frac{2f'}{\beta_1\beta_2} \\ R_2 = \frac{2\alpha_1 f'}{\beta_2(1+\beta_1)} \\ R_3 = \frac{2\alpha_1\alpha_2 f'}{1+\beta_2} \end{cases}, \begin{cases} d_1 = \frac{(1-\alpha_1)f'}{\beta_1\beta_2} \\ d_2 = \frac{\alpha_1(1-\alpha_2)f'}{\beta_2} \\ d_3 = \alpha_1\alpha_2 f' \end{cases}, \tag{6}$$

where R_1, R_2, and R_3 are the radii of curvature of *PM*, *SM*, *TM* respectively, d_1, d_2, and d_3 are the distances between *PM* and *SM*, between *SM* and *TM*, and between *TM* and image plane, respectively.

Then, two value functions of NSGA-II algorithm are constructed, which are image quality evaluation function F_1 and error sensitivity evaluation function F_2. The smaller value of F_1 represents the better image quality of the initial structure corresponding to this set of parameters, and the smaller value of F_2 represents the lower error sensitivity of it corresponding to this set of parameters. The NSGA-II algorithm is used to minimize the two value functions to generate a set of Pareto solutions, where each set of solutions corresponds to one initial structure parameter.

Setting NSGA-II algorithm value function:

(1) Aberration evaluation function F_1

The relationships between the third-order aberration coefficient and the blocking ratio, magnification, and conic coefficient are as follows:

$$\begin{aligned}
S_I = {} & \tfrac{1}{4}\Big[(e_1^2-1)\beta_1^3\beta_2^3 - e_2^2\alpha_1\beta_2^3(1+\beta_1)^3 + e_3^2\alpha_1\alpha_2(1+\beta_2)^3 \\
& +\alpha_1\beta_2^3(1+\beta_1)(1-\beta_1)^2 - \alpha_1\alpha_2(1+\beta_2)(1-\beta_2)^2\Big] \\
S_{II} = {} & -\tfrac{e_2^2(\alpha_1-1)\beta_2^3(1+\beta_1)^3}{4\beta_1\beta_2} - \tfrac{[\alpha_2(\alpha_1-1)+\beta_1(1-\alpha_2)](1+\beta_2)(1-\beta_2)^2}{4\beta_1\beta_2} \\
& +e_3^2\tfrac{[\alpha_2(\alpha_1-1)+\beta_1(1-\alpha_2)](1+\beta_2)^3}{4\beta_1\beta_2} + \tfrac{(\alpha_1-1)\beta_2^3(1+\beta_1)(1-\beta_1)^2}{4\beta_1\beta_2} - \tfrac{1}{2} \\
S_{III} = {} & -e_2^2\tfrac{\beta_2(\alpha_1-1)^2(1-\beta_1^3)}{4\alpha_1\beta_1^2} - \tfrac{[\alpha_2(\alpha_1-1)+(1-\alpha_2)\beta_1]^2(1+\beta_2)(1-\beta_2)^2}{4\alpha_1\alpha_2\beta_1^2\beta_2^2} \\
& -\tfrac{[\alpha_2(\alpha_1-1)+\beta_1(1-\alpha_2)](1-\beta_2)(1+\beta_2)}{\alpha_1\alpha_2\beta_1\beta_2} + \tfrac{\beta_2(1+\beta_1)}{\alpha_1} - \tfrac{1+\beta_2}{a_1\alpha_2} - \beta_1\beta_2 \\
& +e_3^2\tfrac{[\alpha_2(\alpha_1-1)+\beta_1(1-\alpha_2)]^2(1+\beta_2)^3}{4\alpha_1\alpha_2\beta_1^2\beta_2^2} + \tfrac{\beta_2(\alpha_1-1)^2(1+\beta_1)(1-\beta_1)^2}{4\alpha_1\beta_1^2} \\
& -\tfrac{\beta_2(\alpha_1-1)(1-\beta_1)(1+\beta_1)}{\alpha_1\beta_1} \\
S_{IV} = {} & \beta_1\beta_2 - \tfrac{\beta_2(1+\beta_1)}{\alpha_1} + \tfrac{1+\beta_2}{\alpha_1\alpha_2} \\
S_V = {} & \tfrac{2(\alpha_1-1)(\beta_1+1)}{\alpha_1^2\beta_1} + \tfrac{1}{4}\tfrac{(\beta_1+1)(\alpha_1-1)^3(\beta_1-1)^2}{\alpha_1^2\beta_1^3} + \tfrac{3(\alpha_1-1)^2(\beta_1-1)(\beta_1+1)}{2\alpha_1^2\beta_1^2} \\
& +\tfrac{2(\beta_2+1)(\alpha_2-\beta_1-\alpha_1\alpha_2+\alpha_2\beta_1)}{\alpha_1^2\alpha_2^2\beta_1\beta_2} + \tfrac{3(\beta_2-1)(\beta_2+1)(\alpha_2-\beta_1-\alpha_1\alpha_2+\alpha_2\beta_1)^2}{2\alpha_1^2\alpha_2^2\beta_1^2\beta_2^2} \\
& -\tfrac{e_2^2(\alpha_1-1)^3(\beta_1+1)^3}{4\alpha_1^2\beta_1^3} + \tfrac{(\alpha_2-\beta_1-\alpha_1\alpha_2+\alpha_2\beta_1)^3}{4\alpha_1^2\alpha_2^2\beta_1^3\beta_2^3}
\end{aligned} \tag{7}$$

where S_{I}, S_{II}, S_{III}, S_{IV}, and S_{V} are the primary aberration coefficients of spherical aberration, coma, astigmatism, field curvature, and distortion, respectively.

The aberration evaluation function F_1 consists of primary aberration coefficients and weights, as shown in Equation (8).

$$F_1 = \omega_1|S_I| + \omega_2|S_{II}| + \omega_3|S_{III}| + \omega_4|S_{IV}| + \omega_5|S_V|, \tag{8}$$

where ω_1, ω_2, ω_3, ω_4, and ω_5 are the weights corresponding to S_{I}, S_{II}, S_{III}, S_{IV}, and S_{V}, respectively.

(2) Error sensitivity evaluation function F_2

The aberration evaluation function F_2 consists of the error sensitivity of the three mirrors and weights, as shown in Equation (9).

$$F_2 = v_1|SEN_1| + v_2|SEN_2| + v_3|SEN_3|, \tag{9}$$

where SEN_1, SEN_2, and SEN_3 are the error sensitivities of *PM*, *SM*, and *TM*, respectively, and v_1, v_2, and v_3 are the weights corresponding to the error sensitivities of *PM*, *SM*, and *TM*, respectively.

3.2. Desensitization Design Method for Freeform Optical Systems

Based on the above analysis, a design method for freeform TMA optical system with low error sensitivity is proposed.

First, the off-axis angle of the FOV is set according to the FOV requirements, and this step has two purposes: one is to meet the requirements of the FOV, and the other is to make the system unobscured. Set the range of the variables according to the structural parameters of the target optical system. The NSGA-II algorithm is used to obtain a set of Pareto solutions, and the conic TMA optical system with acceptable image quality and error sensitivity is selected from the Pareto solution set as the initial structure for the next optimization.

Then, to further optimize the performance of the TMA system (better image quality and lower error sensitivity), freeform surfaces are used in the design and optimization of the

TMA system. There are many kinds of freeform surface types; choose a variety of surface types from the freeform surface type library to build M freeform TMA systems (if three freeform surface types are selected, and the mirrors are allowed to use the same surface type, the number of constructed systems is 27; if the mirrors are not allowed to use the same surface, the number of systems constructed is 6) in order to study the performance of the freeform TMA optical system with different freeform surface combinations. After all the M systems are optimized, the optical system with the best image quality and lowest error sensitivity is selected as the optimal system output. Different combinations of freeform surface types are compared and discussed with the design results in Section 5.2. The flow chart of the design method of the freeform TMA optical system with low error sensitivity is shown in Figure 4.

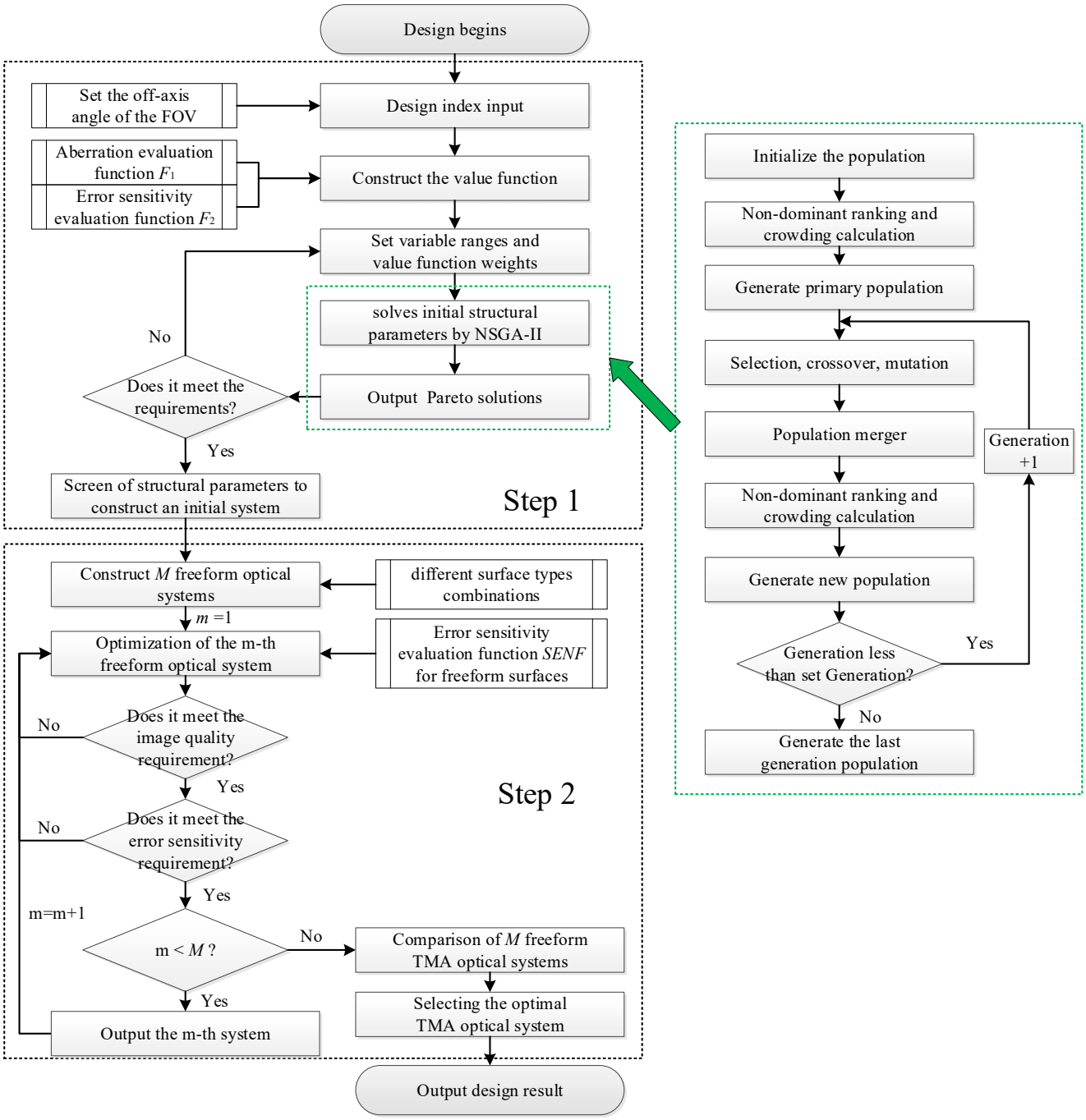

Figure 4. Flow chart of design method of freeform off-axis three-mirror optical system with low error sensitivity.

4. Design Example

A COOK TMA optical system with the focal length of 100 mm, *F*-number of 5, wavelength of 550 nm, square FOV of 3° × 3° (Tangential: −8.5°~−11.5°, Sagittal: −1.5°~1.5°) is designed as an example. The optical system parameters are taken as follows: e_1^2, e_2^2, and e_3^2 are within the range of: −5.0000~5.0000, α_1 is within the range of 0.400~0.500, α_2 is within the range of 1.500~2.000, β_1 is within the range of 1.500~2.000, and β_2 is within the range of 0.350~1.000. Setting all items in the image quality evaluation function and error sensitivity evaluation function is of the same importance. The parameters of the NSGA-II algorithm were set as follows: population size set as 200, the number of iterations set as 500, genetic probability set as 0.9, and variation probability set as 0.1.

The NSGA-II algorithm is used to solve, and the Pareto results are shown in Figure 5, where each ball represents a set of solutions. The projection of all systems on the corresponding surface of the F1-F2 plane is the Pareto front (magenta curve). Three representative systems are selected from 200 sets of results for display. System 21 (orange ball) is the system with better image quality and higher error sensitivity among all systems. On the contrary, System 150 (blue ball) is the system with lower error sensitivity and poorer image quality. In Figure 5, the green dashed box is considered to be systems acceptable to both image quality and error sensitivity. System 174 (purple ball) is a system randomly selected in this area. The image quality of system 174 is better than that of system 150, whereas its error sensitivity is lower than that of system 21. Therefore, system 174 is selected as the initial structure of the freeform TMA optical system. The initial structure parameters of System 21, System 150, and System 174 are shown in Table 1.

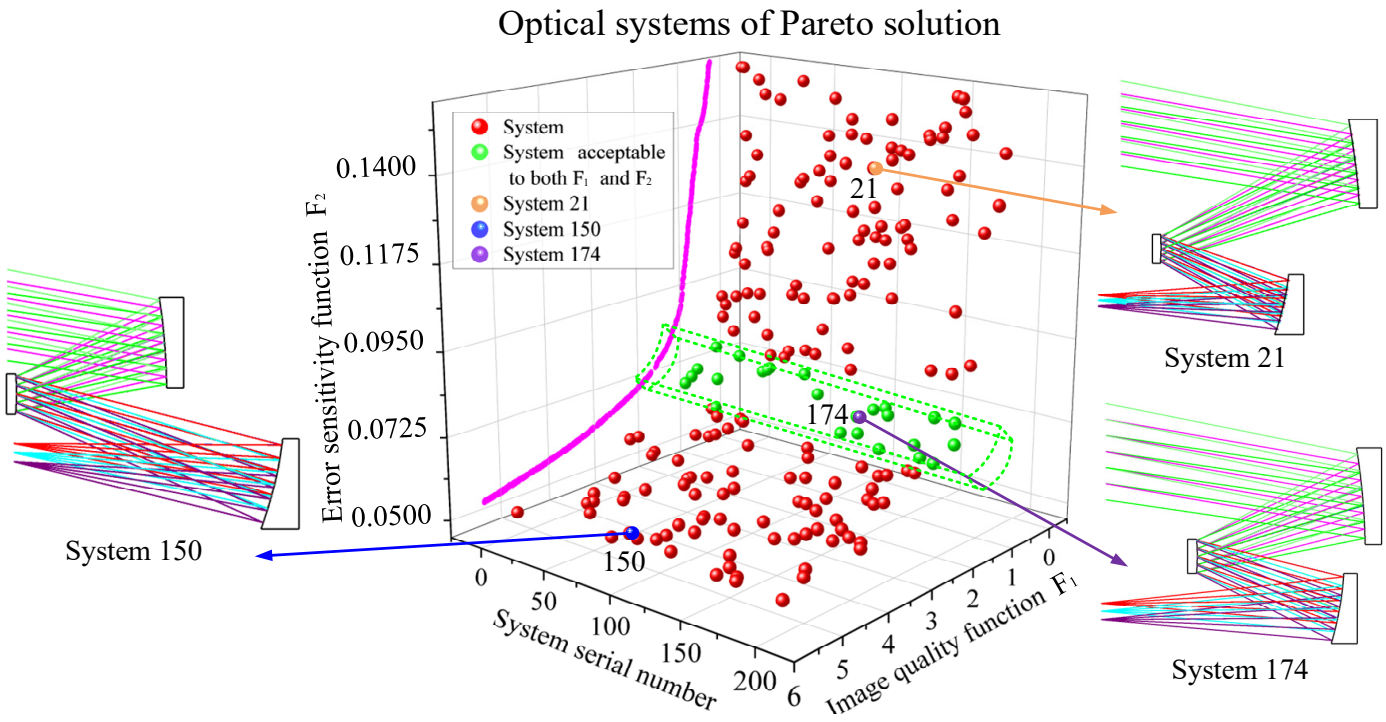

Figure 5. Optical systems of Pareto solution.

Table 1. Initial structure parameters for System 21, System 150, System 174.

System	α_1	α_2	β_1	β_2	e_1^2	e_2^2	e_3^2	F_1	F_2
21	0.431	1.500	1.724	0.500	−1.7066	−0.9001	−0.0228	0.3027	0.1247
150	0.500	1.601	1.999	0.350	−0.6870	−5.0000	0.3202	4.7812	0.0534
174	0.499	1.500	1.748	0.980	−2.3071	0.0900	0.1430	1.0807	0.0728

Next, System 174 was used as the initial structure of the freeform TMA optical system and was optimized. Five Rings and eight Arms (40 reference points) were selected to evaluate and optimize the error sensitivity of the freeform TMA optical system.

In order to compare and select the freeform surface type combination with the best image quality and lowest error sensitivity, we randomly selected three surface types from the freeform surface type library, namely, Fringe Zernike polynomials, *XY* polynomials and Chebyshev polynomials. The general form of a mathematical expression for a freeform surface involves the addition of freeform terms on the basis of a conic surface, as shown in Equation (10):

$$z(x,y) = \frac{c(x^2+y^2)}{1+\sqrt{1-(1+k)c^2(x^2+y^2)}} + \sum_{j}^{J} A_j g_j(x,y), \tag{10}$$

where c is the curvature of the surface, k is the conic coefficient, A_j is the coefficient of the jth freeform term, and $g_j(x,y)$ is the freeform surface term described using polynomials such as Fringe Zernike polynomials or *XY* polynomials.

We use the Fringe Zernike polynomials, Chebyshev polynomials, and *XY* polynomials with the first to fourth order terms. Therefore, the freeform surface terms of *XY* polynomials and Chebyshev polynomials can be provided by Equations (11) and (12):

$$\sum_{j}^{J} A_j g_j(x,y) = \sum_{m=0}^{4}\sum_{n=0}^{4} a_{m,n} x^m y^n, 1 \le m+n \le 4, \tag{11}$$

$$\sum_{j}^{J} A_j g_j(x,y) = \sum_{m=0}^{4}\sum_{n=0}^{4} a_{m,n} t_{m,n}(x,y), 1 \le m+n \le 4, \tag{12}$$

where $t_{m,n}(x,y)$ are subforums of the Chebyshev polynomials. As for the Fringe Zernike polynomials, the freeform surface terms can be provided by Equation (13):

$$\sum_{j}^{J} A_j g_j(x,y) = \sum_{j}^{J} A_j Z_j(\rho,\varphi), j = 2,3,\ldots,13,17,18, \tag{13}$$

where ρ is the normalized radial ray coordinate and φ is the angular ray coordinate.

The six groups of freeform TMA optical systems were constructed according to the application of different freeform surface types to different mirrors for comparison. The image quality threshold of the freeform TMA optical system was set to 0.0200 λ and the error sensitivity threshold was 0.0700. The surface combination and optimization results of the six freeform TMA optical systems are shown in Table 2.

Table 2. Surface combination and optimization results of six groups of freeform TMA optical systems.

System	PM	SM	TM	RMS WFE/λ	$SENF_{system}$
System 174	Conic	Conic	Conic	0.0645	0.0728
System 174-F1	*XY* polynomials	Fringe Zernike polynomials	Chebyshev polynomials	0.0027	0.0687
System 174-F2	*XY* polynomials	Chebyshev polynomials	Fringe Zernike polynomials	0.0081	0.0511
System 174-F3	Fringe Zernike polynomials	*XY* polynomials	Chebyshev polynomials	0.0078	0.0477
System 174-F4	Chebyshev polynomials	Fringe Zernike polynomials	*XY* polynomials	0.0026	0.0266
System 174-F5	Fringe Zernike polynomials	Chebyshev polynomials	*XY* polynomials	0.0200	0.0289
System 174-F6	Chebyshev polynomials	*XY* polynomials	Fringe Zernike polynomials	0.0040	0.0602

Through comparative analysis, System 174-F4 has the best image quality and the lowest error sensitivity, and is considered to be the best system. The layout diagram and Root mean square Wavefront Error (RMS WFE) of System 174-F4 are shown in Figure 6.

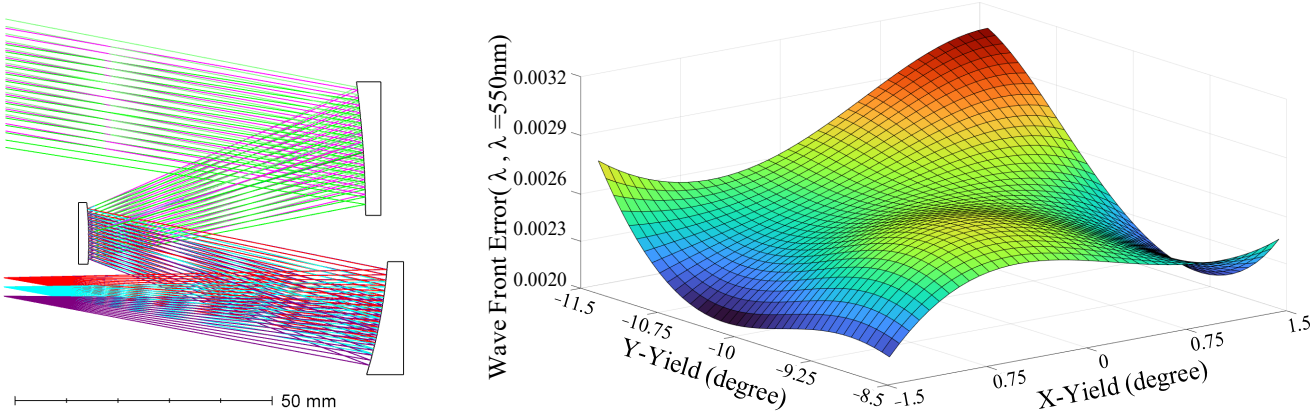

(**a**) (**b**)

Figure 6. Layout and RMS WFE of System 174-F4: (**a**) Layout; (**b**) RMS WFE.

Subsequently, in order to visualize the magnitude of the performance enhancement of TMA optical system by the introduction of the freeform surface, the error sensitivity of conic TMA optical system (System174) and the freeform TMA optical system (System 174-F4), which is considered to be the best combination of the freeform surface types, were analyzed and compared, respectively, and the error sensitivity comparison is as follows in Figure 7.

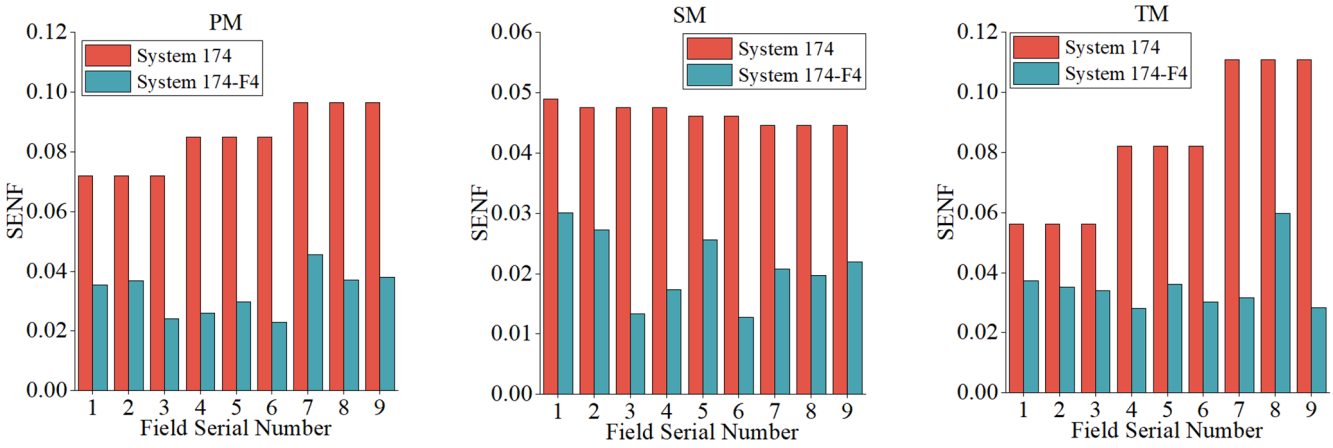

(**a**) (**b**) (**c**)

Figure 7. Error sensitivity analysis of three mirrors of System 174 and System 174-F4: (**a**) *SENF* of *PM*; (**b**) *SENF* of *SM*; (**c**) *SENF* of *TM*.

Error sensitivity analysis was performed for the freeform optical system (System 174-F4) and the conic optical system (System 174). We used the Monte Carlo tolerance analysis method with 500 samples to calculate the average value of ΔRMS WFE. The tilt angle of each mirror is 0.01° and the error amount obeyed a normal distribution. The results are shown in Figure 8.

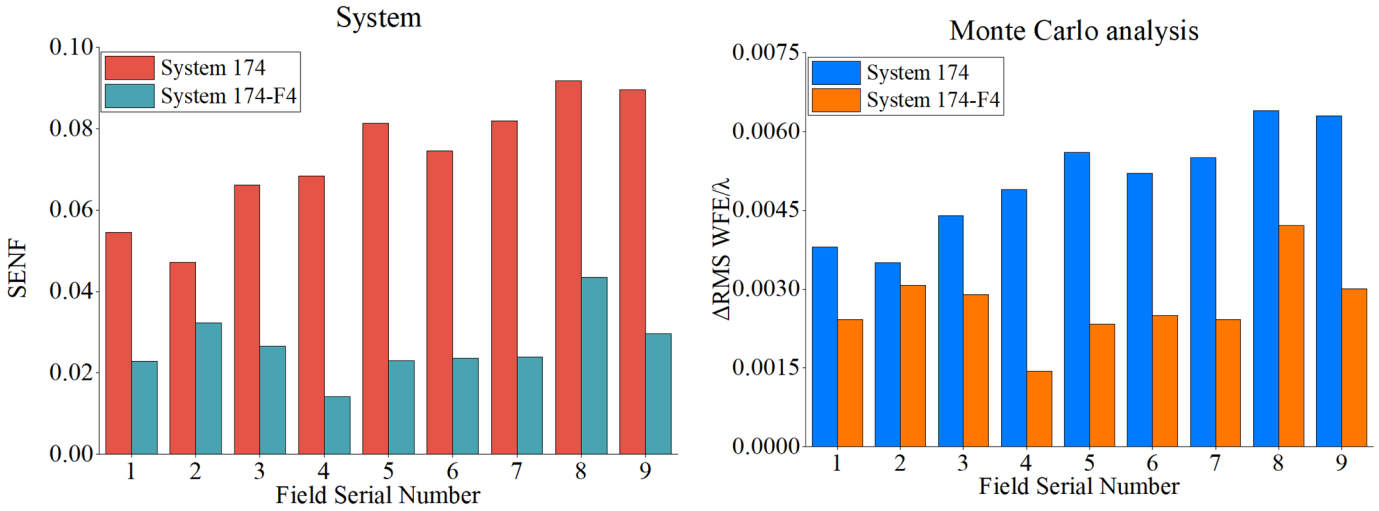

Figure 8. Error sensitivity analysis and Monte Carlo analysis of System 174 and System 174-F4: (**a**) $SENF_{system}$ of System; (**b**) Monte Carlo analysis of System.

The results show that the RMS WFE of conic TMA is 0.0645λ, $SENF_{system}$ is 0.0728, and the average ΔRMS WFE is 0.0049λ when disturbed; the RMS WFE of freeform TMA optimized by desensitization design is 0.0026λ, $SENF_{system}$ is 0.0266, and the average ΔRMS WFE is 0.0025λ when disturbed. Compared with the conic TMA, the RMS WFE of the freeform TMA is 1/25 of the original, and the average ΔRMS WFE is 51% of the original with the same tilt applied, which can prove that our design method is correct and effective.

To illustrate the effectiveness of the low error sensitivity freeform optical system design method proposed in this paper, we add a set of comparisons. System 174-F0 is optimized by the traditional optimization method, and the goal of optimization is the best image quality. During the optimization process, the three mirrors of System 174-F0 were upgraded to freeform surfaces. In order to better compare with System 174-F4 (the best design result using our proposed method), the three mirrors used the same freeform surface types as System 174-F4. After optimization by traditional methods, the RMS WFE of System 174-F0 is 0.0024 λ. Monte Carlo (same parameter settings as System 174-F4) analysis of System 174-F0 shows an average ΔRMS WFE of 0.0040 when disturbed. With the same tilt applied, the ΔRMS WFE of System 174-F4 (the design result using our proposed method) is 62.5% of that of System 174-F0 (the design result not using our proposed method), which can prove that our design method is effective in the optimization design process of freeform TMA optical system.

5. Discussion

5.1. Discussion of Combined Design Methods

In this paper, a combined design method for freeform TMA optical systems is proposed. The NSGA-II algorithm is applied to obtain an initial conic system acceptable to both image quality and error sensitivity. Compared with the traditional "initial structure + DLS algorithm" method, this method obtains a globally optimal solution instead of an optimal local solution, providing an optimal initial structure for further optimization. A good conic optical system as the initial structure of the freeform optical system can be easily optimized to obtain good design results, thus significantly improving the design efficiency. The performance of the system is then continued to be improved by introducing freeform surfaces. The entire design process combines the advantages of the global optimization method, the parameter control method, and the freeform surface optimization method, in which the global optimization method is more suitable for the search of the initial structure and in the subsequent freeform surface optimization process, and the global

optimization method with large sample iterations is not suitable because of the complexity of the freeform surface representation. Therefore, we use the parameter control method to optimize the freeform optical system in the subsequent optimization process. Throughout the design process, we apply different desensitization methods in different steps according to their characteristics, which not only reduces computation time but also obtains good design results. From the design results, the method proposed in this paper is effective.

In addition, when the NSGA-II algorithm is applied to obtain the initial optical system structure parameters, researchers only need to analyze aberration and error sensitivity and set the value function according to the index of the target optical system. The process does not require complex mathematical calculations and program writing, which is simple and easy to implement with good applicability.

5.2. Discussion of Surface Type Combinations and Design Results

As for the design results, as shown in Table 2, the image quality of the freeform TMA optical system is better for the *SM* with Fringe Zernike polynomials and less error sensitive for the *TM* with *XY* polynomials, where the *PM* adopts Chebyshev polynomials, the *SM* adopts Fringe Zernike polynomials, and the *TM* adopts *XY* polynomials as the optimal freeform surface combination. Since Fringe Zernike polynomials is orthogonal in the circular domain, applying it to the *SM* (Stop) can obtain the best imaging quality, which is consistent with the conclusion of Y. Zhong and H. Gross' comparative analysis [36].

In the design comparison process of this paper, the focus is on comparing the design results of different freeform surface types combinations without considering the difficulty of fabrication. In addition, the number of freeform surface types involved in the comparison is small, and in the further study, the number of freeform surface types will be increased and the manufacturing difficulty of different surface types will be considered for a more comprehensive and integrated analysis.

6. Conclusions

The freeform TMA optical system with low error sensitivity can achieve high imaging quality and be highly resistant to error interruptions. In this paper, the existing error-sensitive evaluation function for conic surfaces is extended to the evaluation of freeform surfaces by combining the "Ring-Arm" reference point sampling method. The NSGA-II algorithm is used to establish the initial structure of a good TMA optical system, and then a comprehensive evaluation function that considering the image quality and error sensitivity of the freeform optical system is used to evaluate and compare various combinations of freeform surface types to determine the optimal freeform surface type. As an example, a freeform TMA optical system with a focal length of 100 mm, an *F*-number of 5, and a FOV of $3^\circ \times 3^\circ$ is designed and optimized to use Chebyshev polynomials for the *PM*, Fringe Zernike polynomials for the *SM*, and *XY* polynomials for the *TM*, as the optimal freeform surface combination.

Compared with the conic system (System 174), the image quality of the freeform surface system (System 174-F4) is greatly improved, and the RMS WFE is 1/25 of the original, and the error sensitivity of the three mirrors is greatly reduced with the overall error sensitivity of the system 36.5% of the original. With the same error applied, the ΔRMS WFE is 51% of the original, which verifies the correctness and practicality of the method.

Author Contributions: Conceptualization, Z.Q. and Q.M.; methodology, Z.Q. and Q.M.; software, Z.Q.; validation, Z.Q., Y.Q., C.R. and Q.M.; writing—original draft preparation, Z.Q.; writing—review and editing, Y.Q., C.R. and Q.M.; supervision, X.W. and Q.M.; project administration, X.W. and Q.M. All authors have read and agreed to the published version of the manuscript.

Funding: This research was funded by the Youth Innovation Promotion Association of the Chinese Academy of Sciences (2019219); the National Natural Science Foundation of China (61705220); and the Strategic Priority Research Program of Chinese Academy of Sciences (XDA17010205).

Institutional Review Board Statement: Not applicable.

Informed Consent Statement: Not applicable.

Data Availability Statement: Not applicable.

Conflicts of Interest: The authors declare no conflict of interest. The funders had no role in the design of the study; in the collection, analyses, or interpretation of data; in the writing of the manuscript, or in the decision to publish the results.

References

1. Liu, X.; Gong, T.; Jin, G.; Zhu, J. Design method for assembly-insensitive freeform reflective optical systems. *Opt. Express* **2018**, *26*, 27798–27811. [CrossRef] [PubMed]
2. Meng, Q.; Wang, H.; Wang, K.; Wang, Y.; Ji, Z.; Wang, D. Off-axis three-mirror freeform telescope with a large linear field of view based on an integration mirror. *Appl. Opt.* **2016**, *55*, 8962–8970. [CrossRef] [PubMed]
3. Zhang, X.; Zheng, L.; He, X.; Wang, L.; Zhang, F.; Yu, S.; Shi, G.; Zhang, B.; Liu, Q.; Wang, T. Design and fabrication of imaging optical systems with freeform surfaces. In Proceedings of the Current Developments in Lens Design and Optical Engineering XIII, San Diego, CA, USA, 11 October 2012; p. 848607.
4. Fuerschbach, K.; Rolland, J.P.; Thompson, K.P. A new family of optical systems employing φ-polynomial surfaces. *Opt. Express* **2011**, *19*, 21919–21928. [CrossRef]
5. Reimers, J.; Bauer, A.; Thompson, K.P.; Rolland, J.P. Freeform spectrometer enabling increased compactness. *Light Sci. Appl.* **2017**, *6*, e17026. [CrossRef] [PubMed]
6. Yang, T.; Zhu, J.; Jin, G. Design of free-form imaging systems with linear field-of-view using a construction and iteration process. *Opt. Express* **2014**, *22*, 3362–3374. [CrossRef] [PubMed]
7. Zhu, J.; Hou, W.; Zhang, X.; Jin, G. Design of a low F-number free form off-axis three-mirror system with rectangular field-of-view. *J. Opt.* **2015**, *17*, 015605.
8. Meng, Q.; Wang, H.; Liang, W.; Yan, Z.; Wang, B. Design of off-axis three-mirror systems with ultrawide field of view based on an expansion process of surface freeform and field of view. *Appl. Opt.* **2019**, *58*, 609–615. [CrossRef] [PubMed]
9. Thompson, K. Description of the third-order optical aberrations of near-circular pupil optical systems without symmetry. *J. Opt. Soc. Am. A* **2005**, *22*, 1389–1401. [CrossRef] [PubMed]
10. Meng, Q.; Wang, H.; Wang, W.; Yan, Z. Desensitization design method of unobscured three-mirror anastigmatic optical systems with an adjustment-optimization-evaluation process. *Appl. Opt.* **2018**, *57*, 1472–1481. [CrossRef]
11. Grey, D. Tolerance sensitivity and optimization. *Appl. Opt.* **1970**, *9*, 523–526. [CrossRef]
12. Wassermann, G.D.; Wolf, E. On the Theory of Aplanatic Aspheric Systems. *Proc. Phys. Soc. Sect. B* **1949**, *62*, 2–8. [CrossRef]
13. Zhu, J.; Wu, X.; Yang, T.; Jin, G. Generating optical freeform surfaces considering both coordinates and normals of discrete data points. *J. Opt. Soc. Am. A* **2014**, *31*, 2401–2408. [CrossRef] [PubMed]
14. Hicks, R.A. Controlling a ray bundle with a free-form reflector. *Opt. Lett.* **2008**, *33*, 1672–1674. [CrossRef] [PubMed]
15. Minano, J.C.; Benitez, P.; Lin, W.; Infante, J.; Munoz, F.; Santamaria, A. An application of the SMS method for imaging designs. *Opt. Express* **2009**, *17*, 24036–24044. [CrossRef] [PubMed]
16. Duerr, F.; Benítez, P.; Miñano, J.C.; Meuret, Y.; Thienpont, H. Analytic design method for optimal imaging: Coupling three ray sets using two free-form lens profiles. *Opt. Express* **2012**, *20*, 5576–5585. [CrossRef] [PubMed]
17. Yang, T.; Jin, G.; Zhu, J. Automated design of freeform imaging systems. *Light Sci. Appl.* **2017**, *6*, e17081. [CrossRef] [PubMed]
18. Zhang, B.; Jin, G.; Zhu, J. Towards automatic freeform optics design: Coarse and fine search of the three-mirror solution space. *Light Sci. Appl.* **2021**, *10*, 65. [CrossRef] [PubMed]
19. Yang, T.; Zhu, J.; Hou, W.; Jin, G. Design method of freeform off-axis reflective imaging systems with a direct construction process. *Opt. Express* **2014**, *22*, 9193–9205. [CrossRef] [PubMed]
20. Yang, T.; Zhu, J.; Wu, X.; Jin, G. Direct design of freeform surfaces and freeform imaging systems with a point-by-point three-dimensional construction-iteration method. *Opt. Express* **2015**, *23*, 10233–10246. [CrossRef]
21. Cheng, X.; Wang, Y.; Hao, Q.; Isshiki, M. Global and local optimization for optical systems. *Optik* **2006**, *117*, 111–117. [CrossRef]
22. Vasiljevic, D. Optimization of the Cook triplet with the various evolution strategies and the damped least squares. In Proceedings of the Optical Design and Analysis Software, Denver, CO, USA, 27 September 1999; p. 207.
23. Sturlesi, D.; O'Shea, D.C. The search for a global minimum in optical design. In Proceedings of the Optical Engineering and Commercial Optics, San Diego, CA, USA, 22 December 1989; p. 92.
24. Kuper, T.; Harris, T. A New Look at Global Optimization for Optical Design. *Photonics Spectra* **1992**, *1*, 151–160.
25. Forbes, G.; Jones, A. Global Optimization in Lens Design. *Opt. Photonics News* **1992**, *3*, 23–29. [CrossRef]
26. Sturlesi, D.; O'Shea, D.C. Global view of optical design space. *Opt. Eng.* **1991**, *30*, 207–218. [CrossRef]
27. Isshiki, M.; Gardner, L.; Gregory, G. Automated control of manufacturing sensitivity during optimization. In Proceedings of the Optical Design and Engineering, St. Etienne, France, 18 February 2004; Volume 5249, p. 343.
28. Deng, Y.; Jin, G.; Zhu, J. Design method for freeform reflective-imaging systems with low surface-figure-error sensitivity. *Chin. Opt. Lett.* **2019**, *17*, 092201. [CrossRef]
29. Sasian, J.; Descour, M. Power distribution and symmetry in lens systems. *Opt. Eng.* **1998**, *37*, 1001–1005. [CrossRef]

30. Qin, Z.; Wang, X.; Ren, C.; Qi, Y.; Meng, Q. Design method for reflective optical system with low tilt error sensitivity. *Opt. Express* **2021**, *29*, 43464–43479. [CrossRef]
31. Ma, B.; Sharma, K.; Thompson, K.P.; Rolland, J.P. Mobile device camera design with Q-type polynomials to achieve higher production yield. *Opt. Express* **2013**, *21*, 17454–17463. [CrossRef]
32. Thompson, K.P.; Schiesser, E.; Rolland, J.P. Why are freeform telescopes less alignment sensitive than a traditional unobscured TMA? In Proceedings of the Optifab 2015, Rochester, New York, USA, 11 October 2015; Volume 9633, p. 963317.
33. Fuerschbach, K.; Davis, G.E.; Thompson, K.P.; Rolland, J.P. Assembly of a freeform off-axis optical system employing three φ-polynomial Zernike mirrors. *Opt. Lett.* **2014**, *39*, 2896–2899. [CrossRef]
34. Wang, L.; Sasian, J. Merit figures for fast estimating tolerance sensitivity in lens systems. In Proceedings of the International Optical Design Conference 2010, Jackson Hole, WY, USA, 9 September 2010; Volume 7652, p. 76521P.
35. Deb, K.; Pratap, A.; Agarwal, S.; Meyarivan, T. A Fast and Elitist Multiobjective Genetic Algorithm: NSGA-II. *IEEE Trans. Evol. Comp.* **2002**, *6*, 182–197. [CrossRef]
36. Zhong, Y.; Gross, H.; Broemel, A.; Kirschstein, S.; Petruck, P.; Tuennermann, A. Investigation of TMA systems with different freeform surfaces. In Proceedings of the Optical Systems Design 2015: Optical Design and Engineering VI, Jena, Germany, 23 September 2015; Volume 9626, p. 96260X.